

Supporting Figures

Structural analysis of the P132L disease mutation in caveolin-1 reveals its role in assembly of oligomeric complexes

Bing Han^{1,2}, Alican Gulsevin³, Sarah Connolly⁴, Ting Wang^{1,2}, Brigitte Meyer², Jason Porta⁴, Ajit Tiwari^{1,2}, Angie Deng⁵, Louise Chang⁴, Yekena Peskova^{1,2}, Hassane S. Mchaourab⁵, Erkan Karakas⁵, Melanie D. Ohi^{4,7}, Jens Meiler^{3,6}, and Anne K. Kenworthy^{1,2,*}

¹ Center for Membrane and Cell Physiology, University of Virginia, Charlottesville, VA USA.

² Department of Molecular Physiology and Biological Physics, University of Virginia School of Medicine, Charlottesville, VA, USA

³ Department of Chemistry, Vanderbilt University Nashville, TN, USA

⁴ Life Sciences Institute, University of Michigan, Ann Arbor, MI, USA.

⁵ Department of Molecular Physiology and Biophysics, Vanderbilt University Nashville, TN, USA

⁶ Institute for Drug Discovery, Leipzig University, Germany

⁷ Department of Cell and Developmental Biology, University of Michigan School of Medicine, Ann Arbor, MI, USA

*To whom correspondence should be addressed. Akk7hp@virginia.edu

Running title: Structural basis for the P132L mutation in caveolin-1

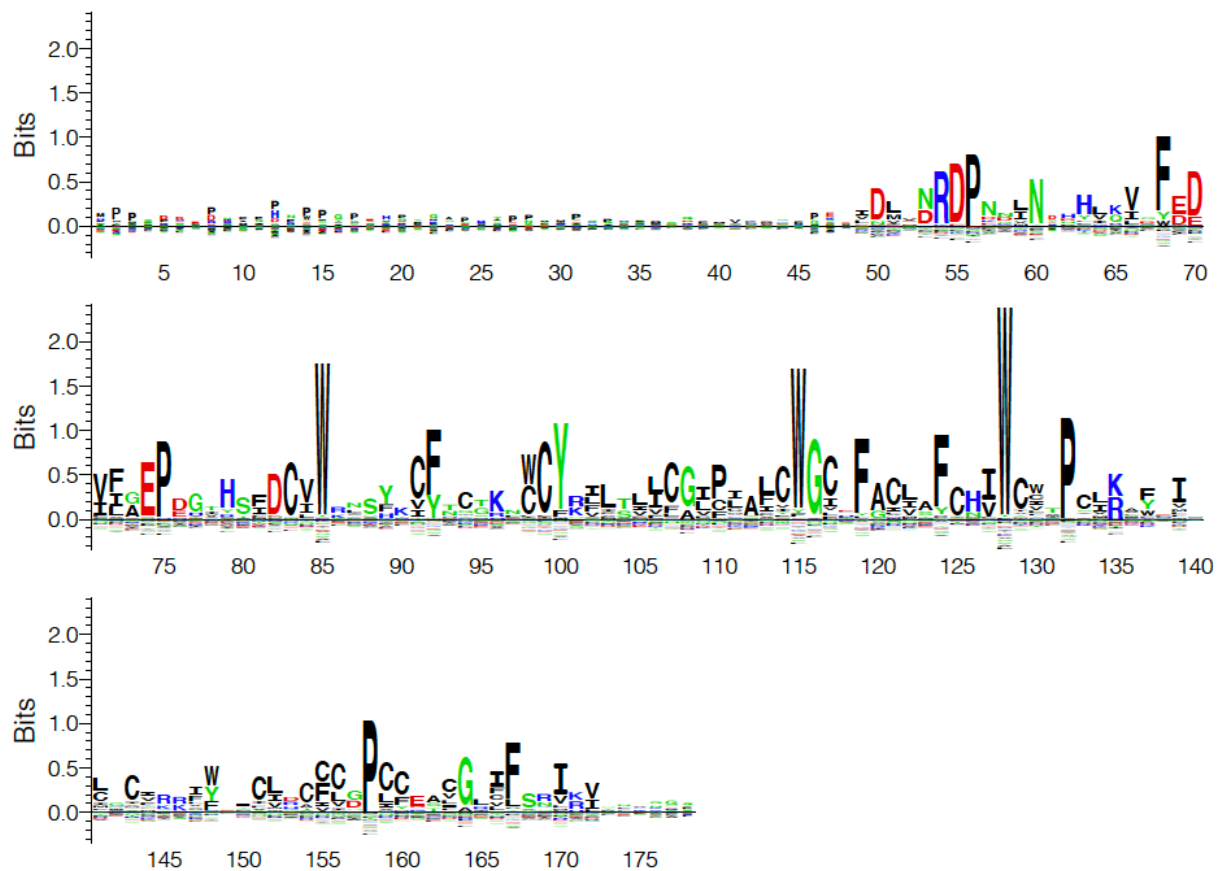


Figure S1. Sequence logo of CAV1 among metazoan caveolins. Logo was created with Seq2Logo.

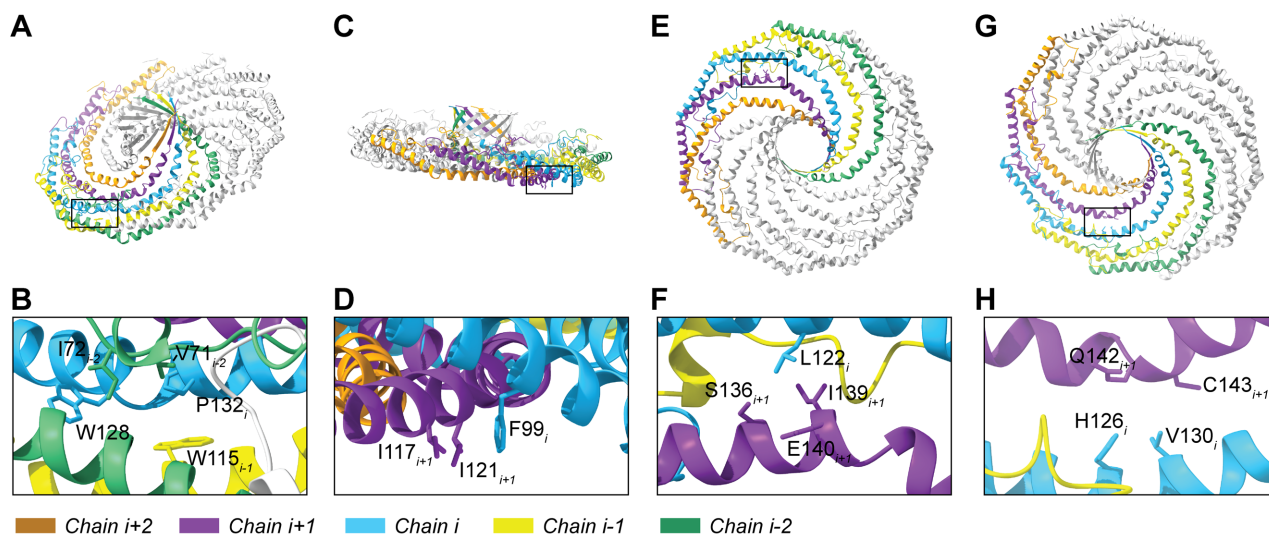


Figure S2. Positions of P132, F99, L122, and V130 in the CAV1 complex. Chains are color coded as follows: $i+2$, brown; $i+1$, purple; i , cyan; $i-1$, yellow, and $i-2$, green. (A, B) P132. (C, D) F99. (E, F) L122. (G, H) V130.

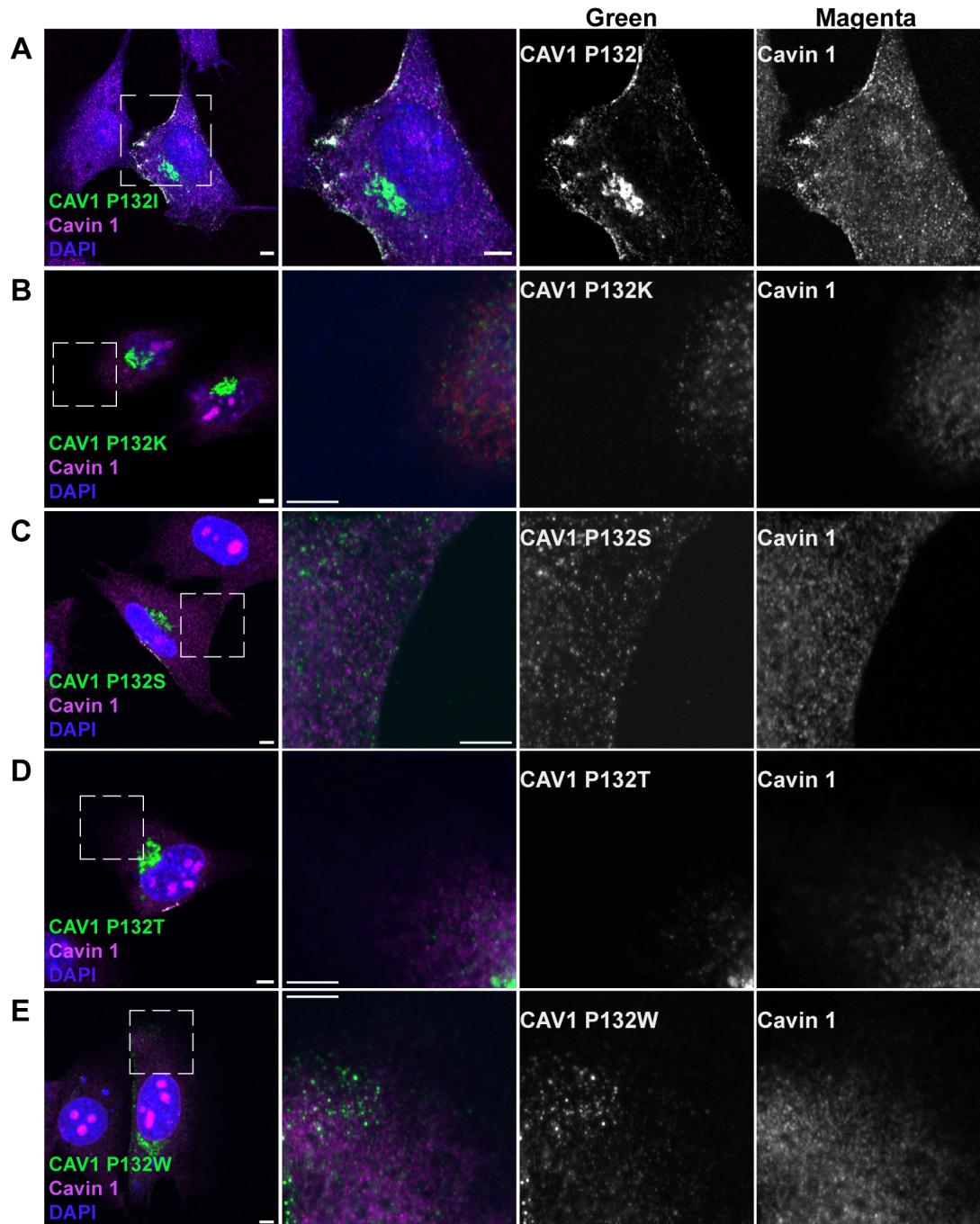


Figure S3. Single amino acid substitutions to P132 cause CAV1 to accumulate in the Golgi complex. Representative confocal images are shown for CAV1^{-/-} MEF cells expressing myc-tagged (A) P132I, (B) P132K, (C) P132S, (D) P132T, and (E) P132W. Cells were allowed to express the indicated constructs for 24h, fixed, and immunostained for endogenous cavin-1 (magenta) and myc (green) prior to imaging. Dashed boxes indicate position of zoomed images highlighting the low levels of staining outside of the Golgi complex. Note that low levels of plasma membrane staining are observed for P132I in addition to a substantial Golgi pool. Bars, 5 μ m.

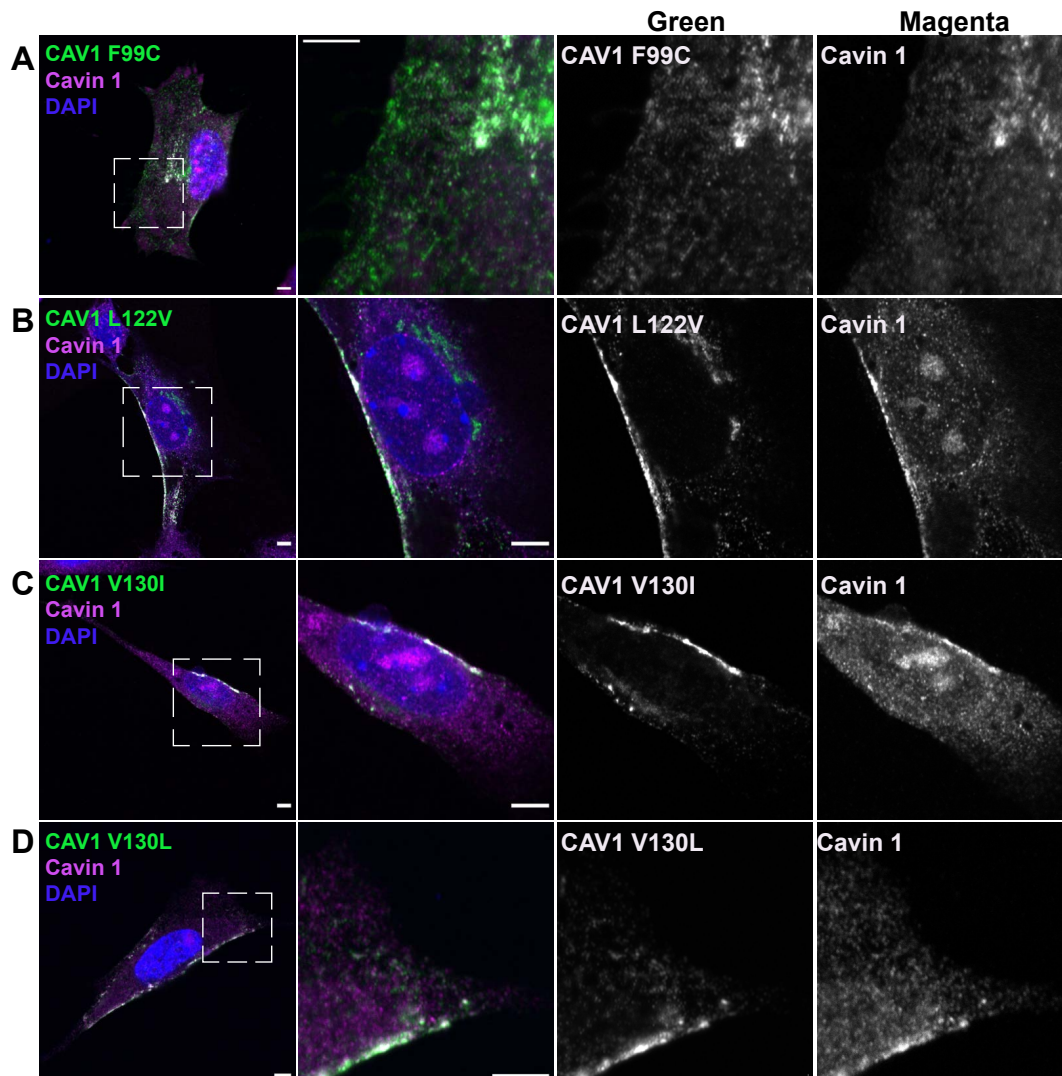


Figure S4. Single amino acid substitutions to F99, L122, or V130 do not interfere with the delivery of CAV1 to the plasma membrane. Representative confocal images are shown for CAV1^{-/-} MEF cells expressing myc-tagged (A) F99C, (B) L122V, (C) V130I, and (D) V130L. Cells were allowed to express the indicated constructs for 24h, fixed, and immunostained for endogenous cavin-1 (magenta) and myc (green) prior to imaging. Dashed boxes indicate position of zoomed images highlighting cell surface pools of CAV1 that colocalize with cavin-1. Bars, 5 μ m

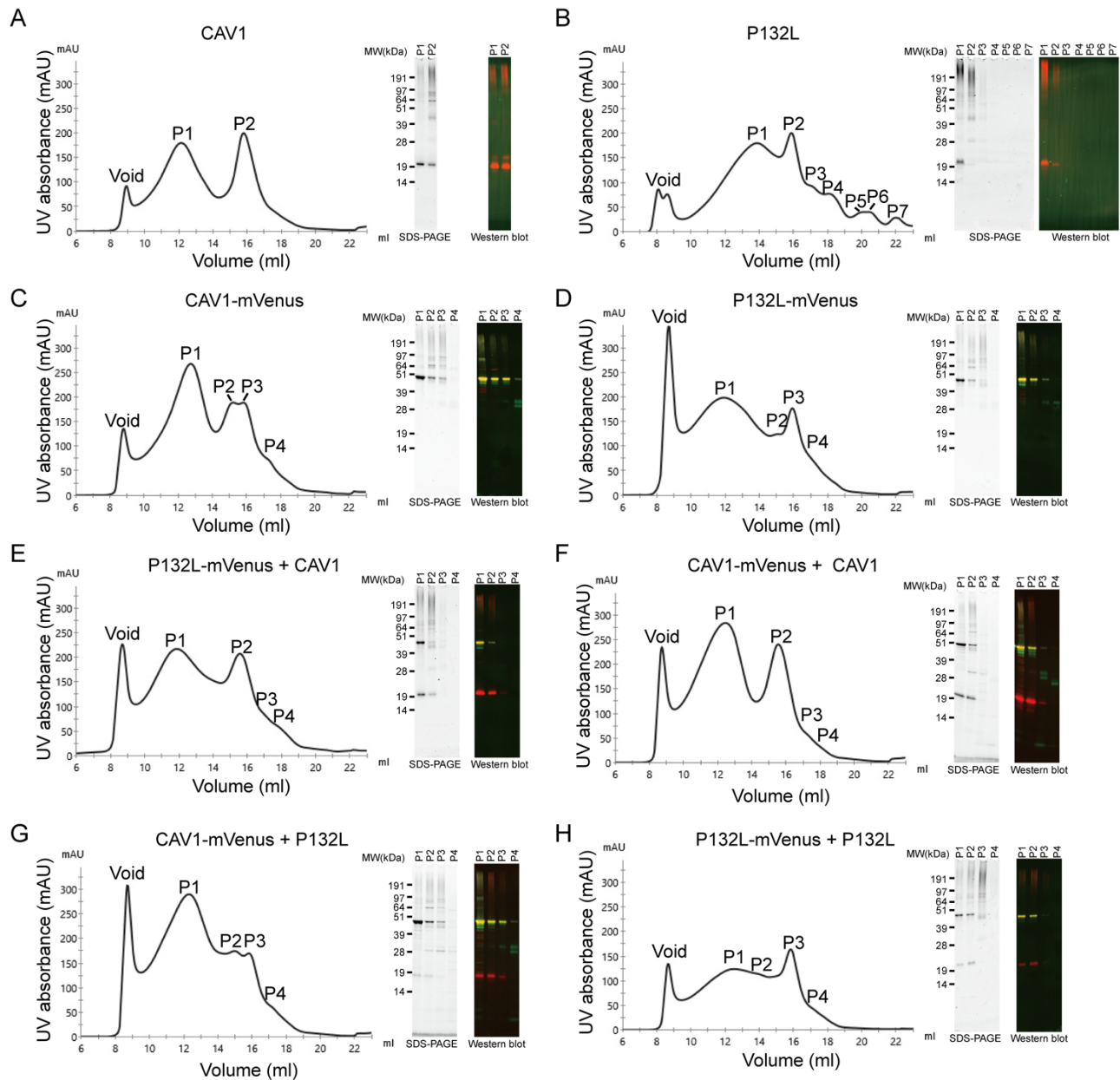


Figure S5: FPLC traces, SDS-PAGE electrophoresis and Western blotting of CAV1 constructs used in this study. The indicated Cav1 proteins were purified from *E. coli* membranes and applied to a Superose®6 10/300 GL column. Elution profiles, SDS-PAGE and Western blotting results are shown for (A) CAV1, (B) P132L, (C) CAV1-mVenus, (D) P132L-mVenus, (E) co-expressed P132L-mVenus and CAV1, (F) co-expressed CAV1-mVenus and CAV1, (G) co-expressed CAV1-mVenus and P132L, and (H) co-expressed P132L and P132L-mVenus. In the Western blotting results, mVenus signal is shown in green and CAV1 signal is in red.

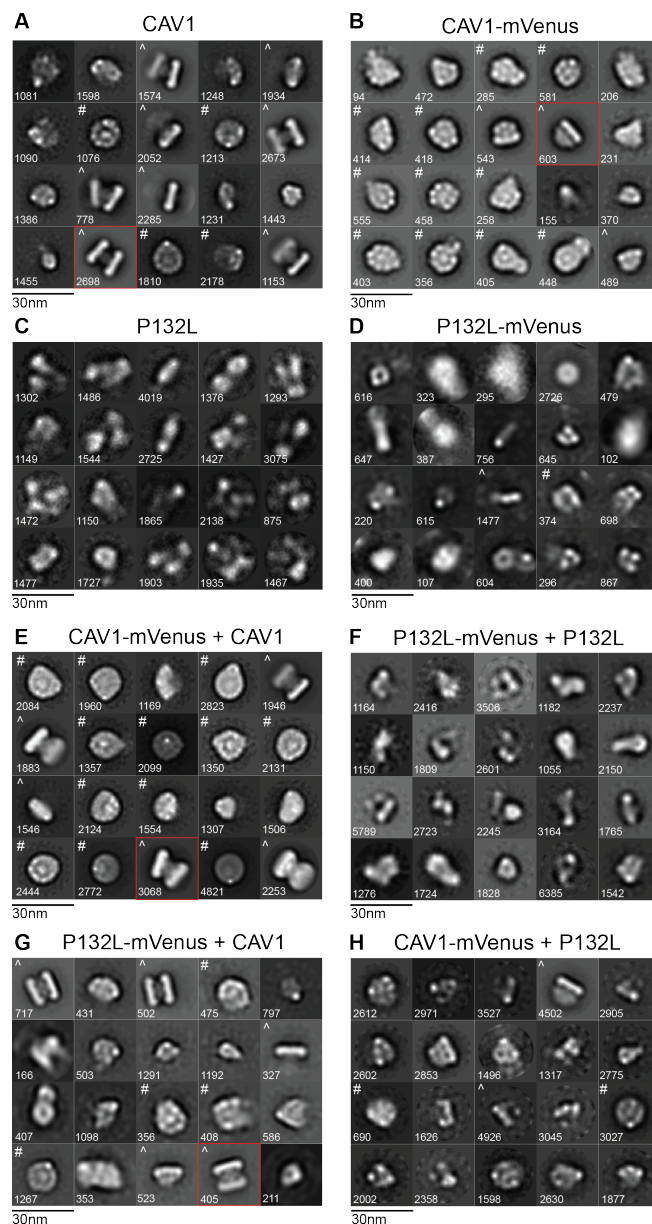


Figure S6: Negative stain averages of Cav1 constructs. Negative stain class averages of (A) CAV1, (B) CAV1-mVenus, (C) P132L, (D) P132L-mVenus, (E) co-expressed CAV1-Venus and CAV1 (F), co-expressed P132L-mVenus and P132L, (G) co-expressed P132L-mVenus and CAV1, and (H) co-expressed CAV1-Venus and P132L. # denotes en face averages, ^ denotes side view averages, and the number of particles per average are noted in the bottom left. Scale bars, 30 nm. Classes in red boxes are displayed in Figure 7.

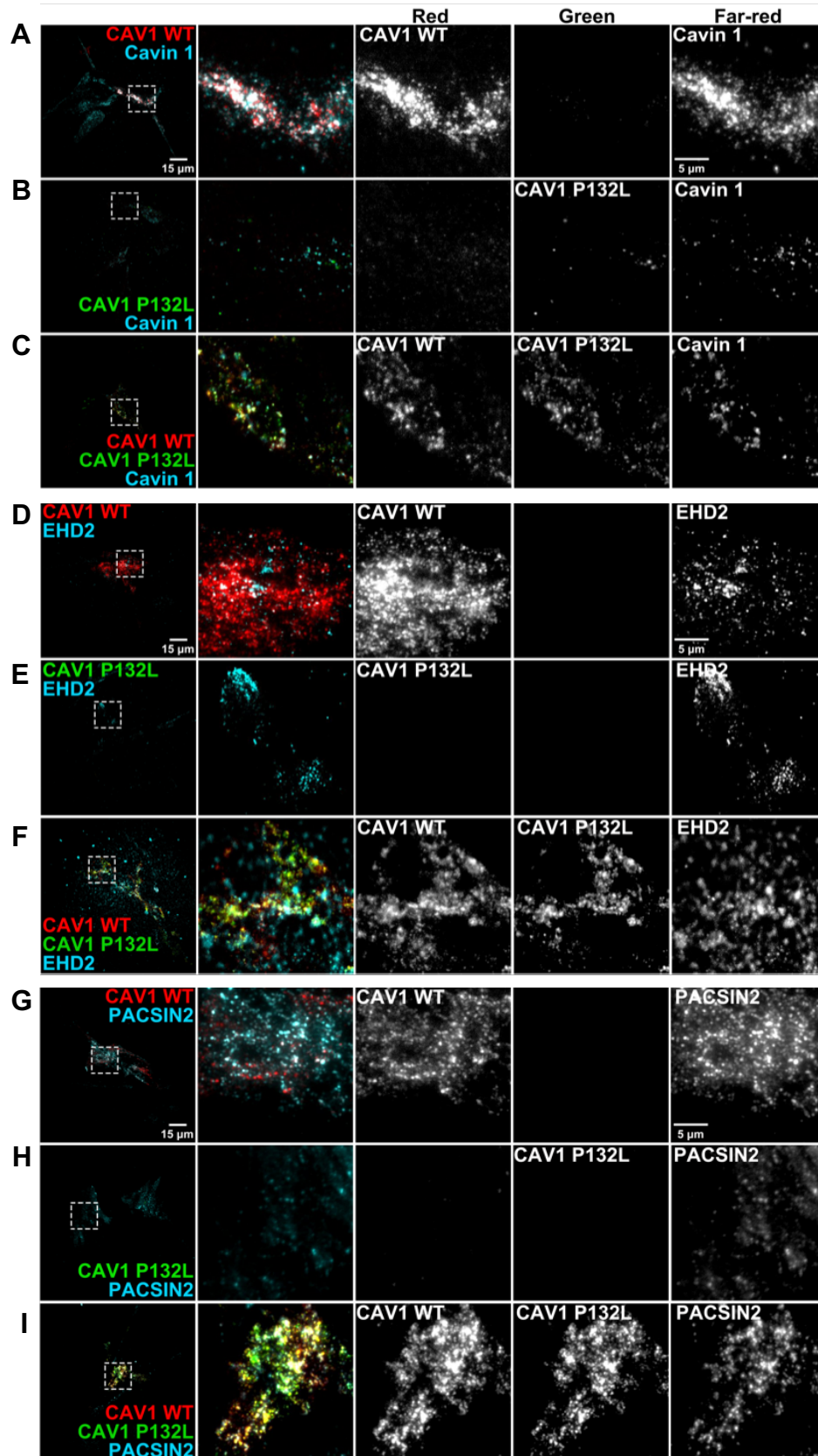


Figure S7. When co-expressed with WT CAV1, P132L is recruited to cell surface puncta that partially co-localize with endogenous cavin-1, EHD2, and PACSIN-2 in CAV1^{-/-} MEFs as visualized using TIRF microscopy.

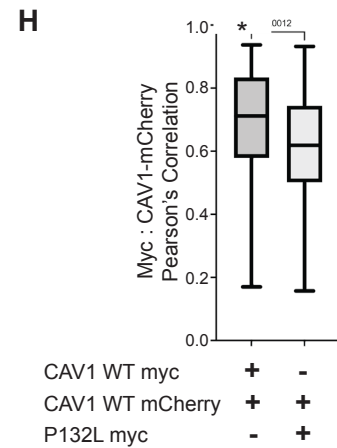
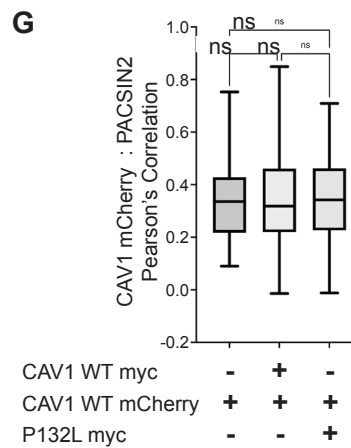
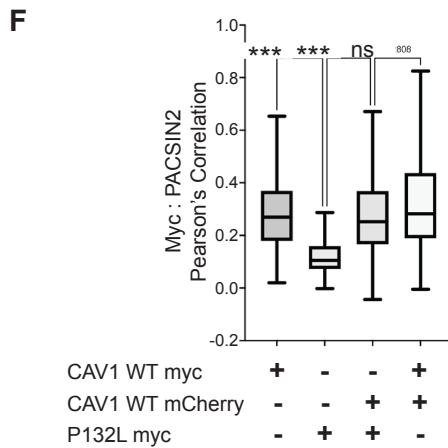
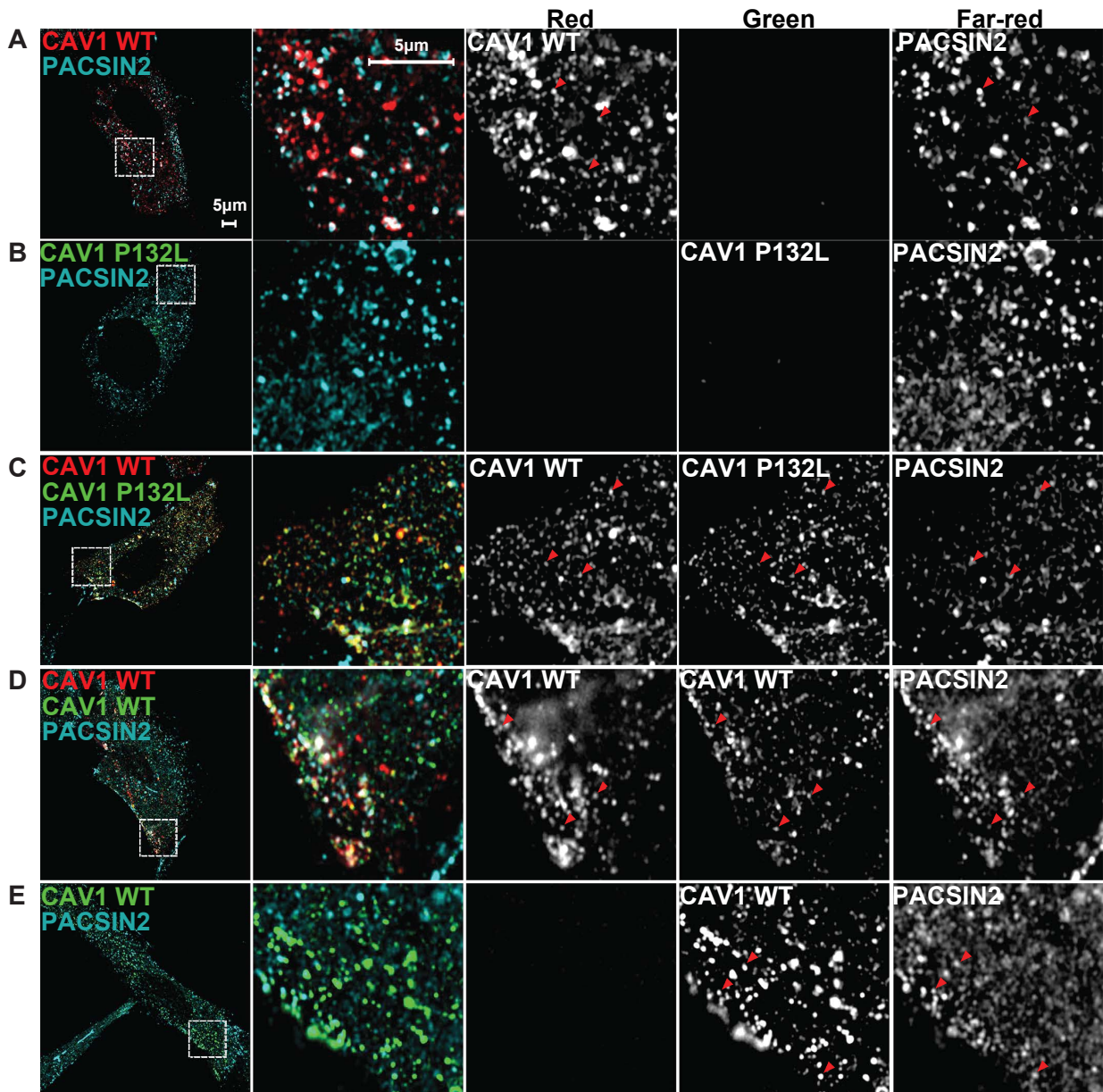


Figure S8. When co-expressed with WT CAV1, P132L partially co-localizes with endogenous PACSIN2. CAV1^{-/-} MEFs were transiently transfected with **(A)** CAV1-mCherry, **(B)** P132L, **(C)** CAV1-mCherry plus P132L, **(D)** CAV1-mCherry plus CAV1, or **(E)** CAV1 for 24h, fixed, and immunostained prior to imaging. Representative AiryScan images are shown. Bar, 5 μ m. **(F-H)** Pearson's correlation analysis was carried out using ImageJ (n = 90 ROIs from 3 independent experiments). A one-way ANOVA with Tukey's test (≥ 3 groups) or an unpaired Student's t test (2 groups) was used to calculate P-values. n.s., not significant.

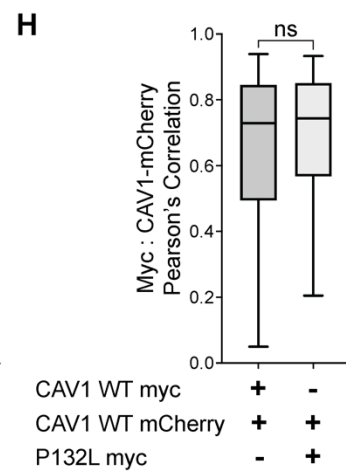
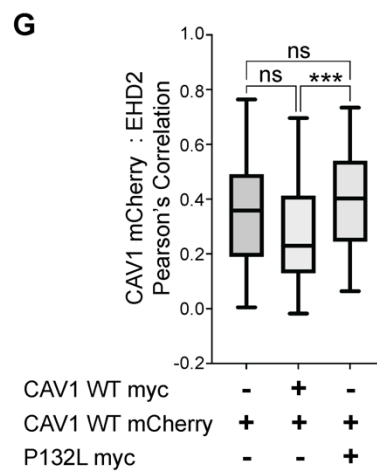
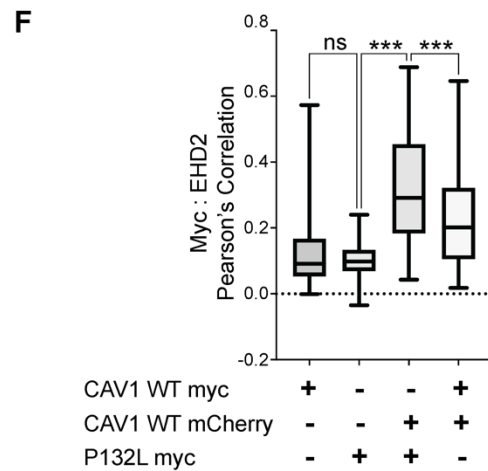
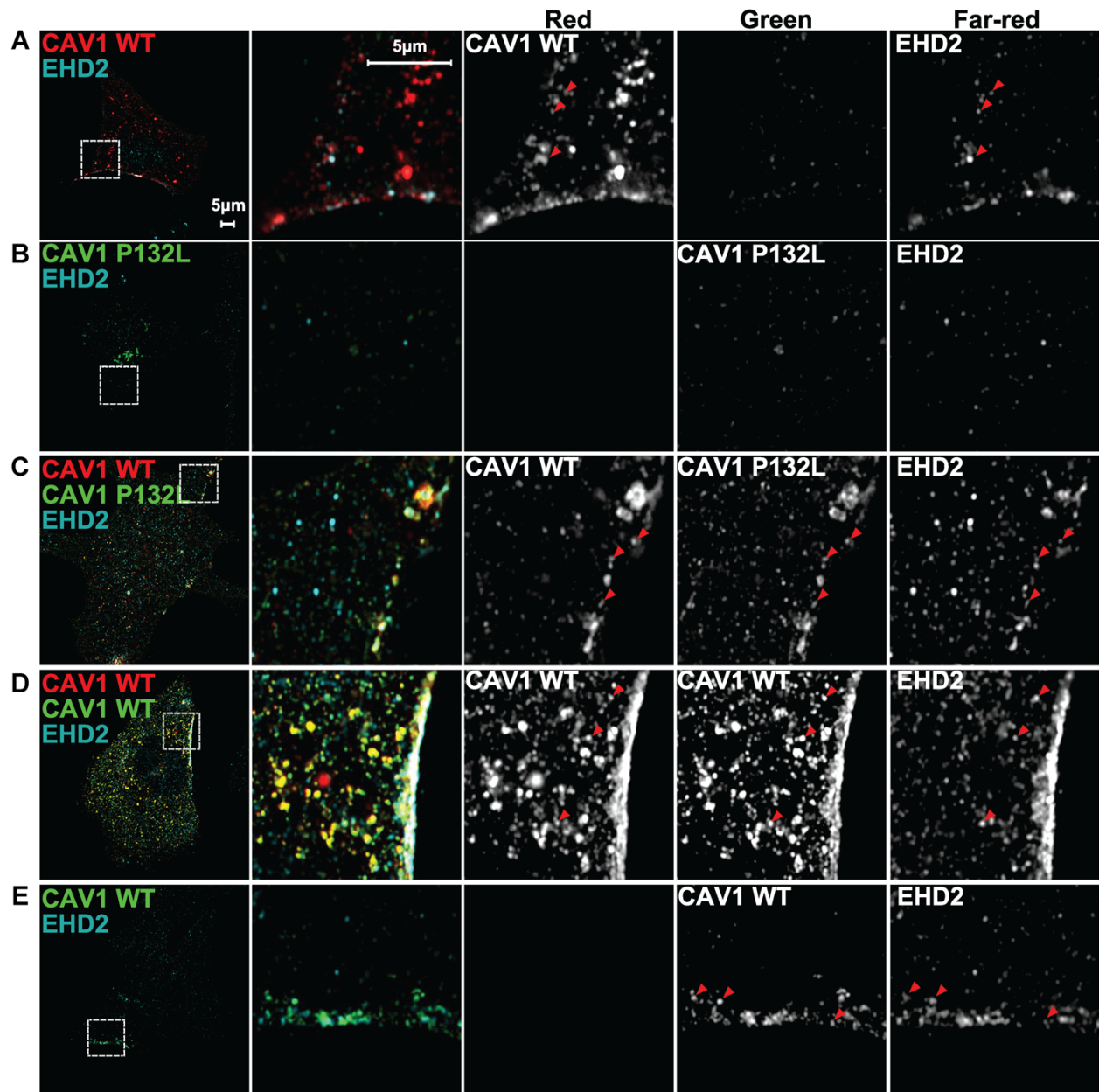


Figure S9. P132L partially colocalizes with endogenous EHD2 when co-expressed with WT CAV1. CAV1^{-/-} MEFs were transiently transfected with **(A)** CAV1-mCherry, **(B)** P132L, **(C)** CAV1-mCherry plus P132L, **(D)** CAV1-mCherry plus CAV1, or **(E)** CAV1 for 24h, fixed, and immunostained prior to imaging. Representative AiryScan images are shown. Bar, 5 μ m. **(F-H)** Pearson's correlation analysis was carried out using ImageJ (n = 90 ROIs from 3 independent experiments). A one-way ANOVA with Tukey's test (≥ 3 groups) or an unpaired Student's t test (2 groups) was used to calculate P-values. n.s., not significant.